Visible Light Crosslinking of Gelatin Hydrogels Offers an Enhanced Cell Microenvironment with Improved Light Penetration Depth

Khoon S. Lim[1,2,3*], Barbara J. Klotz[2,3], Gabriella C. J. Lindberg[1,2], Ferry P. W. Melchels[4], Gary J. Hooper[1], Jos Malda[3,5,6], Debby Gawlitta[2,3], Tim B. F. Woodfield[1,2,3*]

[1]Christchurch Regenerative Medicine and Tissue Engineering (CReaTE) Group, Department of Orthopaedic Surgery and Musculoskeletal Medicine, University of Otago Christchurch, Christchurch 8011, New Zealand.

[2]Medical Technologies Centre of Research Excellence, New Zealand

[3]Maurice Wilkins Centre for Molecular Biodiscovery, New Zealand

[4]Department of Oral and Maxillofacial Surgery & Special Dental Care, University Medical Center Utrecht, Utrecht, The Netherlands

[5]Regenerative Medicine Center Utrecht, Utrecht, The Netherlands.

[6]Institute of Biological Chemistry, Biophysics and Bioengineering, Heriot-Watt University, Edinburgh, United Kingdom

[7]Department of Orthopaedics, University Medical Center Utrecht, Utrecht, The Netherlands

[8]Department of Equine Sciences, Faculty of Veterinary Medicine, Utrecht University, Utrecht, The Netherlands

*Corresponding authors, khoon.lim@otago.ac.nz, tim.woodfield@otago.ac.nz

Abstract

In this study, we investigated the cyto-compatibility and cellular functionality of cell-laden gelatin-methacryloyl (Gel-MA) hydrogels fabricated using a set of photo-initiators which absorb in 400 – 450 nm of the visible light range. Gel-MA hydrogels crosslinked using this combination of visible light photo-initiators, which consisted of ruthenium (Ru) and sodium persulfate (SPS), were characterised to have comparable physico-mechanical properties (sol fraction, mass swelling ratio and compressive modulus) as Gel-MA gels photo-polymerised using more conventionally adopted photo-initiators, such as 1-[4-(2-hydroxyethoxy)-phenyl]-2-hydroxy-2-methyl-1-propan-1-one (Irgacure® 2959) and lithium phenyl(2,4,6-trimethylbenzoyl) phosphinate (LAP). We demonstrated that the Ru/SPS system had a less adverse effect on the viability and metabolic activity of human articular chondrocytes encapsulated in Gel-MA hydrogels for up to 35 days. Furthermore, cell-laden constructs crosslinked using the Ru/SPS system had significantly higher glycosaminoglycan (GAG) content, and re-differentiation capacity as compared to cells embedded in gels crosslinked using UV + I2959 and Vis + LAP. We also demonstrated that the Vis + Ru/SPS system offered significantly greater light penetration depth as compared to the UV + I2959 system, allowing thick (10mm) Gel-MA hydrogels to be fabricated with homogenous crosslinking density throughout the construct. These results demonstrate the potential of these Ru/SPS visible light photo-initiators for use in fabricating cell-laden hydrogels, which offer considerable advantages over traditional UV polymerising systems in terms of clinical relevance and practicability for applications such as cell encapsulation, 3D constructs for tissue engineering, biofabrication and *in situ* crosslinking of injectable hydrogels.

1. Introduction

In recent years, scaffold-based strategies adopting hydrogels as biomaterials for tissue engineering have received significant attention and offer a number of advantages due to their highly hydrated polymeric network and their structural similarity to native extracellular matrix [1]. Among these, photo-polymerisable gelatin hydrogels are especially attractive as they offer the ability for spatial and temporal control over the polymerisation process. Additionally, the reaction can be performed at room or physiological temperature, with fast curing rates and minimal heat generation [2,3].

In general, the photo-polymerisation process requires grafting of functional photo-labile moieties, such as methacryloyl (methacrylamides and methacrylates), tyramine, or styrene to gelatin [4–10]. Amongst these different photo-crosslinkable gelatin materials, gelatin-methacryloyl (Gel-MA) has emerged as a promising biomaterial, due to the tailorable physical properties (crosslinking density, swelling and stiffness) depending on the degree of methacryloyl substitution and the initial macromer concentration, thereby making it a versatile platform for various tissue engineering applications [4,11]. To date, the most commonly used photo-initiator to crosslink Gel-MA is 1-[4-(2-hydroxyethoxy)-phenyl]-2-hydroxy-2-methyl-1-propan-1-one, which is also known as Irgacure® 2959 (I2959) [12,13]. When exposed to ultraviolet (UV) light, Gel-MA undergoes crosslinking through chain-growth radical polymerisation. Here, the I2959 molecules absorb photons of light and dissociate into radicals, which then propagate through the methacryloyl groups, forming covalent kinetic chains to hold the polymer chains together (Figure 1A) [13].

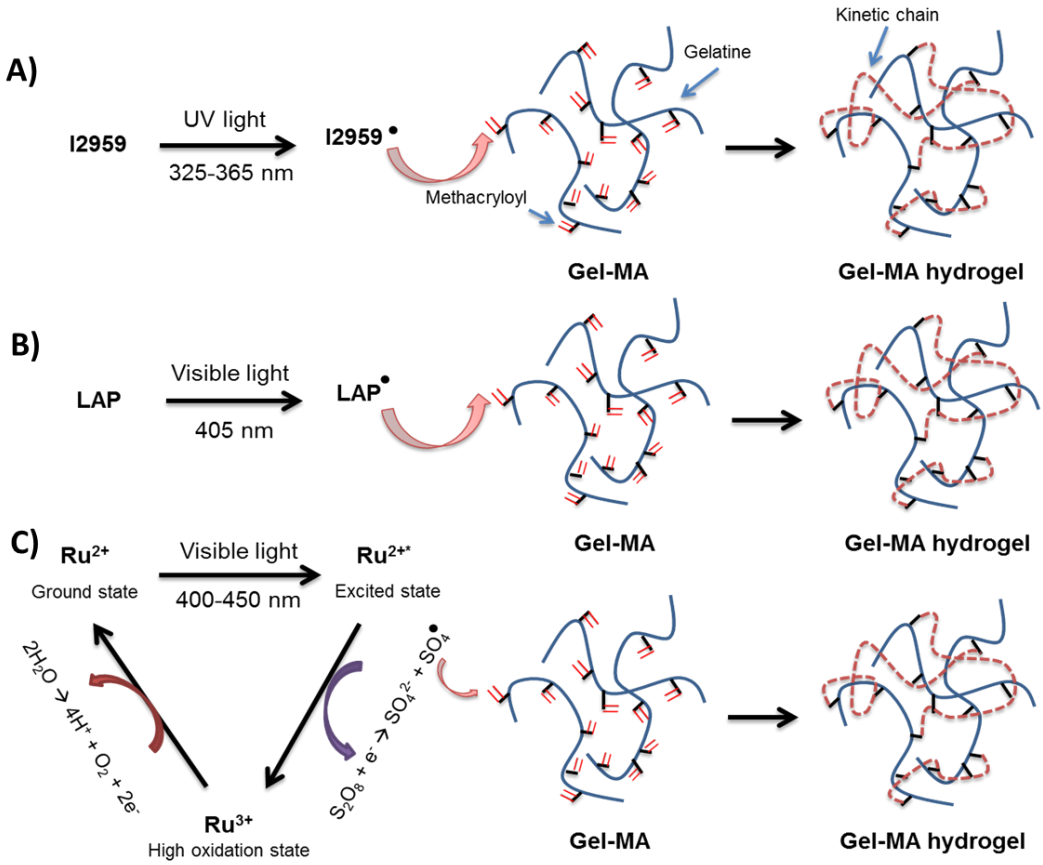

Figure 1: Schematic of the Gel-MA crosslinking process using A) UV light and I2959; B) Visible light and LAP; C) Visible light and Ru/SPS.

However, one major drawback of using I2959 is that it requires ultraviolet (UV) light for photo-excitation, which can potentially cause cellular DNA and tissue damage [14–16]. For example, previous studies conducted by Dahle *et al.* demonstrated that both UVA (320 – 400 nm) and UVB (290 – 320 nm) radiation can induce chromosomal, as well as genetic instability in mammalian cells [17,18]. Furthermore, Lavker *et al.* reported that repetitive exposure of human skin to low dose of UVA resulted in dermal alternations such as inflammation and lysozyme deposition [19]. UV light can also react with oxygen in the environment, forming reactive oxygen species (ROS), such as the superoxide radical ($O_2^{\cdot -}$), hydroxyl radical ($OH^{\cdot}$), singlet oxygen ($^1O_2$) and ozone (O_3), which have also been shown to cause oxidative damage to DNA [19,20]. Additionally, for *in vivo* injectable hydrogel applications, UV light has been previously reported to have limited light penetration depth and can be attenuated by the native tissue

[21,22]. Elisseeff *et al.* showed that transmittance of UVA through human skin was significantly reduced, where visible light photo-initiating systems were more efficient for transdermal polymerisation [23]. Therefore, the development and cell-related characterisation of alternative photo-polymerisation systems that operate in the visible light (400-700 nm) spectrum may offer significant advantages for tissue engineering applications such as cell delivery or as space-fillers post augmentation, compared to more common UV photo-polymerisation.

To date, a number of visible light photo-initiating systems have been investigated to fabricate cell-laden Gel-MA hydrogels, and include: camphorquinone [24,25], fluorescein [24], rose bengal [26], riboflavin [24], lithium phenyl-2,4,6-trimethylbenzoylphosphinate (LAP) [27,28], and eosin Y [29]. In particular, LAP behaves very similarly to I2959, both being type 1 photo-initiators that undergo unimolecular bond cleavage to generate free radicals to facilitate polymerisation (Figure 1B) [14,27]. However, LAP has limited molar absorptivity in a narrow visible light range ($\varepsilon \sim 30\ M^{-1}cm^{-1}$ at 405 nm), resulting in the need of using high concentrations to fabricate hydrogels [14,27]. On the other hand, although eosin-Y has a much higher molar absorptivity ($\varepsilon \sim 100{,}000\ M^{-1}cm^{-1}$ at 525 nm), it often requires the presence of both a co-initiator (triethanoloamine) and a co-monomer (N-vinylpyrrolidinone or N-vinylcaprolactam) to facilitate methacryloyl based photo-polymerisation [30–33]. In contrast, another emerging visible light initiating system, consisting of a ruthenium (Ru)-based transition metal complex ($\varepsilon \sim 14600\ M^{-1}cm^{-1}$ at 450 nm) and sodium persulfate (SPS), has shown potential for tissue engineering applications [34–37]. When irradiated with visible light, the photo-excited Ru^{2+} oxidises into Ru^{3+} by donating electrons to SPS (Figure 1B). After accepting electrons, SPS dissociates into sulphate anions and sulphate radicals (Figure 1B). These radicals are subsequently able to crosslink Gel-MA by propagating through the methacryloyl groups [38], [39]. However, the cellular functionality such as cell differentiation

and tissue formation in cell-laden constructs photo-crosslinked using this Ru/SPS visible light system has not been investigated. Moreover, the feasibility of this visible light photo-initiating system to allow fabrication of large and thick constructs for *in situ* photo-curing has also not been demonstrated.

Therefore, the aim of this study was to assess cyto-compatibility and cell functionality of cell-laden Gel-MA hydrogels fabricated using the Ru/SPS visible light photo-initiating system. We describe herein the systematic characterisation of physical properties of the visible light cross-linked Gel-MA hydrogels over a range of photo-initiator concentrations and irradiation conditions, compared to the two conventional and most commonly adopted systems, UV + I2959 and Vis + LAP. With clinical translation of this system in mind, we also evaluated the light penetration depth of the Ru/SPS system to assess the feasibility of developing thick, fully-crosslinked tissue engineered constructs while maximising cell viability. Given that one of the potential applications of cell-encapsulated visible light cross-linked Gel-MA hydrogels is in cartilage tissue engineering, we investigated the *in vitro* re-differentiation capacity of expanded human articular chondrocytes as a clinically relevant cell source for further characterisation of the Ru/SPS system.

2. Materials and methods

2.1. Materials

Gelatin (porcine skin, type A, 300g Bloom strength), phosphate buffered saline (PBS), methacrylic anhydride, cellulose dialysis membrane (14 kDa molecular weight cut-off), L-ascorbic acid-2-phosphate (AsAp), tris(2,2-bipyridyl)dichlororuthenium(II) hexahydrate (Ru), sodium persulfate (SPS), calcein-AM, Propidium Iodide (PI), proteinase K, dimethyl-methylene blue (DMMB), ethylenediaminetetraacetic acid disodium salt dihydrate (Di-sodium-EDTA), sodium chloride (NaCl), hyaluronidase, ITS+1, dexamethasone, ,

hydrochloric acid (37%), sodium hydroxide (NaOH), chondroitin sulphate A (CS-A) and L-proline were purchased from Sigma-Aldrich (Missouri, USA). 1-[4-(2-hydroxyethoxy)-phenyl]-2-hydroxy-2-methyl-1-propan-1-one (Irgacure® 2959) was a gift from BASF (Ludwigshafen, Germany). Collagenase type II was purchased from Worthington biochemical corporation (Lakewood, USA). Lithium phenyl-2,4,6-trimethylbenzoylphosphinate (LAP) was purchased from Toyo Chemical Industry (Tokyo, Japan). Dulbecco's Modified Eagle's Medium (DMEM) high glucose, 4-(2-hydroxyethyl)-1-piperazine-ethanesulfonic acid (HEPES), Gibco non-essential amino acids (NEAA), foetal calf serum (FCS), 0.25% trypsin/EDTA, and penicillin-streptomycin (PS, 10,000 U/mL), AlamarBlue® reagent, bovine serum albumin (BSA), goat-anti-mouse secondary antibody (Alexa Fluor 488), F-actin rhodamine phalloidin (Alexa Fluor® 594 Phalloidin), 4,6-diamidino-2-phenylindole (D1306, DAPI), and the CyQUANT® cell proliferation assay kit were purchased from ThermoFisher Scientific (Auckland, New Zealand). Medical grade silicone sheets were obtained from BioPlexus (Ventura, USA). Cell strainers (100 µm) were purchased from BD Biosciences (Auckland, New Zealand). Di-sodium hydrogen phosphate (Na_2HPO_4) and acetic acid (glacial, 100%) was ordered from Merck Millipore (Darmstadt, Germany). Optimal cutting temperature compound (OCT) was obtained from VWR International (Auckland, New Zealand). Transforming growth factor β 1 (TGFβ-1) was purchased from R&D systems, Minneapolis, USA. Primary antibodies collagen II (II-II6B3-C) were purchased from DSHB (Iowa City, USA). Primary antibodies for collagen I (Ab34710) and aggrecan (Ab3773) were obtained from Abcam (Melbourne, Australia).

2.2. Synthesis of gelatin-methacryloyl (Gel-MA)

Gelatin was dissolved in PBS at a 10wt% concentration, with 0.6 g of methacrylic anhydride per gram of gelatin added to the solution, and left to react for 1 h at 50˚C under constant stirring [4]. This was followed by dialysis against deionised water to remove unreacted

methacrylic anhydride. The purified Gel-MA solution was filtered through a 0.22 µm sterile filter, then lyophilised under sterile conditions. The degree of methacryloyl substitution was quantified to be 60% (data not shown) using ^{1}H-proton nuclear magnetic resonance spectroscopy (Bruker Avance 400 MHz).

2.3. Fabrication of Gel-MA hydrogels

Dried sterile Gel-MA (10wt%) was dissolved in PBS at 37˚C and left to cool overnight at RT. Prior to crosslinking, the Gel-MA solution was heated to 37˚C, then Ru and SPS were added, scooped into the silicon moulds (5 mm diameter x 1 mm thickness) on a glass slide and sandwiched with a cover slip. The samples were then irradiated (20 cm distance from light source for all experiments) under light (OmniCure® S1500, Excelitas Technologies). The light was irradiated through a light filter (Rosco IR/UV filter) where only light of the wavelength 400 – 450 nm and final intensity of 30 mW/cm^2 was allowed to pass through. A variety of initiator concentrations (0.1/1, 0.2/2 and 0.3/3 of Ru/SPS (mM/mM)) and exposure times (0.5, 1, 3, 5, 10 and 15 minutes) were studied to optimise the irradiation conditions. Gel-MA hydrogels fabricated using Vis (intensity = 30 mW/cm^2, 400 - 450 nm) + 0.05wt% LAP, UV (intensity = 30 mW/cm^2, 300 - 400 nm) + 0.05wt% I2959, and a variety of exposure times (0.5, 1, 3, 5, 10 and 15 minutes) were used as controls.

2.3.1. Swelling and mass loss analysis

All samples were weighed for the initial wet mass ($m_{initial,\ t0}$) after crosslinking, and three samples were lyophilised immediately to obtain their dry weights ($m_{dry,\ t0}$). The actual macromer fraction was calculated based on the equation below:

$$Actual\ macromer\ fraction = \frac{m_{dry,\ t=0}}{m_{initial,\ t=0}} \quad (1)$$

These samples were then submerged in a bath of PBS and incubated at 37°C. Samples were removed from the incubator after 1 day, blotted dry and weighed ($m_{swollen}$). The swollen samples were then freeze-dried and weighed again (m_{dry}). The sol fraction and mass swelling ratio (q) were calculated as follows:

$$m_{initial,dry} = m_{initial}\ x\ actual\ macromer\ fraction \quad (2)$$

$$Sol\ fraction\ = \frac{m_{initial,dry} - m_{dry}}{m_{initial,dry}}\ x\ 100\% \quad (3)$$

$$q = \frac{m_{swollen}}{m_{dry}} \quad (4)$$

2.3.2. Compression testing

The stiffness of the fabricated hydrogels was measured at room temperature using a dynamic mechanical analyser (TA instruments, DMA 2980). Unconfined compression testing was performed at 30% strain/min (5 mm diameter x 2 mm thickness) and the corresponding force was measured at a sampling frequency of 1.67 Hz. Sample diameter was measured using vernier callipers, and the compressive modulus was calculated from the slope of the linear region (10-15% strain range) of the stress-strain curves as previously reported [7].

2.4. Cartilage excision, chondrocyte isolation and expansion

Healthy human articular cartilage was harvested following ethics approval (New Zealand Health and Disability Ethics Committee - URB/07/04/014) from a consenting 28 year old female patient undergoing ligament reconstruction of the knee. The cartilage was diced into 1 to 2 mm^3 cubes and digested overnight at 37˚C with 0.15% w/v collagenase type II in basic chondrocyte medium (DMEM high glucose medium supplemented with 10% FCS, 10 mM HEPES, 0.2 mM L-ascorbic acid-2-phosphate, 0.4 mM L-proline and 1% Penicillin/Streptomycin). The resulting suspension was filtered through a 100-µm cell strainer to exclude the undigested tissue and centrifuged at 700g for 4 min. Isolated human articular

chondrocytes (HACs) were cultured in basic chondrocyte medium and expanded at 37°C in a humidified 5% CO_2/95% air incubator. Media was refreshed twice per week.

2.5. HAC encapsulation in Gel-MA hydrogels

Expanded HACs at P2 were trypsinised and suspended in basic chondrocyte medium. The cell suspension was added to the macromer solution containing sterile filtered initiators to give a final concentration of 5 x 10^6 HACs/ml. The cell-laden gels were then fabricated as outlined previously in section 2.3. Samples were then irradiated for 15 minutes at an intensity of 30 mW/cm^2 for both UV and visible light, where initiator concentrations were kept at 0.05wt% I2959, 0.05wt% LAP or 0.2/2 (mM/mM) Ru/SPS respective to the light source. Constructs were cultured in chondrogenic differentiation media (Dulbecco's DMEM high glucose supplemented with 0.4 mM L-proline, 10 mM HEPES, 0.1 mM NEAA, 100 U/mL penicillin, 0.1 mg/mL streptomycin, 0.2 mM AsAp, 1 x ITS+1 premix, 1.25 mg/mL BSA, 10 nM dexamethasone and 10 ng/mL TGFβ-1). Live/dead, AlamarBlue®, glycosaminoglycan (GAG) and DNA assays were performed on the samples after 1, 21, 35 days in culture as described below.

2.6. Live/dead assay

Harvested samples were washed with PBS, then stained with 1 µg/ml of Calcein-AM and 1 µg/ml of PI for 10 minutes. Live cells stained green whereas dead cell nuclei stained red. After staining, the gels were washed with PBS for three times before imaging them, using a fluorescence microscope (Zeiss Axio Imager Z1). The number of live and dead cells were quantified using the ImageJ software (Bio-Formats plugin) and the cell viability was calculated using the equation below:

$$Viability\ (\%) = \frac{number\ of\ live\ cells}{number\ of\ live\ cells + dead\ cells}\ x\ 100\% \quad (5)$$

2.7. AlamarBlue® assay

An AlamarBlue assay was performed to determine the metabolic activity of cells according to the manufacturer's protocol. Samples were incubated in basic chondrocyte medium containing 10% (v/v) AlamarBlue® reagent for 24 hours. The AlamarBlue® reagent is reduced from blue to red/pink colour by metabolically active cells. The reduction in AlamarBlue® reagent was calculated after measuring the absorbance at 570 nm, using 600 nm as a reference wavelength (Fluostar Galaxy BMG Labtechnology).

2.8. Glycosaminoglycan (GAG) and DNA assay

Glycosaminoglycan (GAG) and DNA content were measured as described previously [3,40]. Briefly, cell-laden Gel-MA samples were digested overnight in 200 µL of 1 mg/ml proteinase-K solution at 56 ˚C. In order to quantify the amount of GAG retained in the gel, the digested samples were reacted with DMMB dye. The absorbance was then measured on a plate reader at 520 nm (Fluostar Galaxy BMG Labtechnology). GAG content was calculated from a standard curve constructed using known concentrations of chondroitin sulphate-A. The DNA content in the gels was measured using a CyQUANT kit. Following digestion, cells were lysed and RNA degraded using the provided lysis buffer with RNase A (1.35 KU/ml) added for 1 hour at RT. GR-dye solution was then added to the samples, incubated at RT for 15 minutes, then the fluorescence was measured (Fluostar Galaxy BMG Labtechnology). A standard curve was constructed using the DNA provided in the kit.

2.9. Immunofluorescence histological examination

The cell-laden constructs were fixed in 10% formalin for 1 hour at RT and washed in PBS supplemented with 0.1 M glycine. For histological evaluation, the samples were embedded in OCT then cryo-sectioned (30 µm thick sections) [8, 32]. Sections were incubated in

0.1 wt.-% hyaluronidase for 30 min at RT, washed with PBS and blocked with 2 wt.% bovine serum albumin (BSA) in PBS for 1 hour at RT. Primary antibodies for collagen type I (1:200, rabbit), collagen type II (1:200, mouse) or aggrecan (1:300, mouse), were diluted in blocking buffer and applied overnight at 4 ºC. Samples were washed three times in blocking buffer for 10 min each followed by incubation with a goat-anti-mouse (Alexa Fluor® 488) and donkey-anti-rabbit (Alexa Fluor® 594) secondary antibodies, diluted in blocking buffer (1:400), in the dark for 1 hour at RT. For the last 10 min of the incubation, 4',6-Diamidino-2-Phenylindole, Dihydrochloride (DAPI, 1:1000 dilution) was added. Lastly, constructs were washed three times in PBS and visualised using the Zeiss Axioimager Z1 microscope.

2.10. Gene expression

Samples cultured for 1 week were collected, digested in 10mg/ml proteinase K solution at 55°C for 30 min, incubated with 1ml TRIzol regent for 5 min at RT followed by RNA isolation in accordance with the manufacturer's guidelines. In brief, 200 µl of chloroform was vigorously mixed with the samples, followed with 3 min RT incubation and 15 min centrifugation at 12000 g. The aqueous phase containing the RNA was transferred to tubes containing 500 µl isopropanol then incubated at RT for 20 min followed by centrifugation for 10 min at 12000 g. The RNA pellet was washed twice in cold 70% ethanol and re-suspended in RNase free water. Ambion® DNA-free™ DNase Treatment was further used to remove any contaminating DNA according to manufacturer's instructions. Total RNA yield was determined using a spectrophotometer (Thermo Scientific, NanoDrop 8000) and the integrity was validated electrophoretically (Agilent Technologies, 2200 TapeStation). 300 ng total RNA per sample was reverse transcribed into complementary DNA (cDNA) using TaqManTM first strand synthesis. Polymerase chain reaction (PCR) was then performed using an iCycler quantitative real-time PCR (qRT-PCR) machine (Roche, LightCycler®480 II), SYBRGreen™ and primers (Sigma Aldrich, KiCqStart® SYBR® Green Primers. The specific genes of

interest were collagen type IA1 (GenBank accession no NM_000088), collagen type IIA1 (GenBank accession no NM_001844) and aggrecan (GenBank accession no NM_001135). Glyceraldehyde-3-phosphate dehydrogenase (GAPDH, Sigma Aldrich, GenBank accession no NM_002046) was selected as housekeeping gene. Each sample was run in duplicate and the threshold cycle and primer efficiency were analysed, where the geometric mean of the reference gene (GAPDH) was used to calculate the normalised mRNA expression of each target gene.

2.11. Light penetration depth study

10wt% Gel-MA macromers were prepared as outlined above in section 2.3. Prior to crosslinking, Ru and SPS were added to the Gel-MA solution for a final concentration of 0.2/2 (mM/mM) Ru/SPS, pipetted into silicon moulds (5 mm diameter x 10 mm thickness) on a glass slide and sandwiched with a cover slip. The samples were then irradiated under light (OmniCure® S1500, Excelitas Technologies) for 15 minutes through a light filter (Rosco IR/UV filter) where only light of 400 – 450 nm wavelength and final intensity of 30 mW/cm^2 was allowed to pass through. Gel-MA hydrogels fabricated using UV light (intensity = 30 mW/cm^2, 300 – 400 nm), 0.05wt% I2959 and 15 minutes of exposure time were used as controls. The fabricated hydrogels were then carefully removed from the mould and sliced into five 2mm thick sections and marked as regions (i to v) relative to the depth from the irradiation source. The sections were then subjected to mass loss and swelling studies as outlined in section 2.3.1. A similar setup was also adopted to fabricate HAC-laden constructs, with subsequent live/dead analysis (section 2.7) performed to evaluate cell viability within each of the five regions (i to v) relative to the depth from the irradiation source.

2.12. Transdermal polymerisation and *in vivo* subcutaneous implantation

Gel-MA hydrogels fabricated using either UV + I2959 or Vis + Ru/SPS were implanted subcutaneously in BALB/C mice as per ethics approval C3/16. All hydrogel macromer components were sterile filtered prior to usage, the samples were crosslinked sterilely in a laminar flow hood, and incubated in sterile PBS overnight prior to implantation. Female BALB/C mice were anaesthetised using inhalational isofluorane. After shaving and disinfection, subcutaneous pockets of approximately 10mm deep were made by blunt dissection in a ventral direction from the incision down the side of the mouse in both directions. The pre-fabricated sterile Gel-MA hydrogels were then inserted into the base of the subcutaneous pocket, and the incision was closed using sutures and surgical glue. After 14 days, the mice were sacrificed and the implants with surrounding tissue and underlying muscle were carefully dissected from the subcutaneous site and fixed in 4% (v/v) phosphate buffered formalin for at least 1 day at 4 °C. The harvested samples were then cryo-sectioned (30 µm sections) and stained with haematoxylin (H) and eosin (E). For imitation of transdermal polymerisation, the mice were shaven after sacrificed, the skin from the dorsal region was harvested, and tissue hydration was maintained in a saline bath. 10wt% Gel-MA macromer solution with either 0.2/2 (mM/mM) Ru/SPS or 0.05wt% I2959 were pipetted into silicon moulds (5 mm diameter x 10 mm thickness) on a glass slide and sandwiched with a cover slip. The harvested skin sample were then placed on top of the samples, and light (OmniCure® S1500, Excelitas Technologies) was allowed to irradiate through the skin for 15 minutes to crosslink the samples. A final intensity of 30 mW/cm^2 was used for both the UV and visible light systems. Hydrogels fabricated with the same conditions without being covered by skin were used as controls. The fabricated hydrogels were then carefully removed from the mould and subjected to mass loss analysis as outlined in section 2.3.1.

2.13. Statistical analysis

All results were analysed using a two-way ANOVA with post-hoc Tukey's multiple comparisons tests unless stated. Data for mass loss and swelling studies were analysed using a one-way ANOVA. The models were constructed using GraphPad Prism (GraphPad Software, version 6). Samples in each study were all prepared in triplicate, and all studies were repeated 3 times ($n=3$). A $p<0.05$ was considered as statistically significant.

3. Results

3.1. Fabrication of Gel-MA hydrogels

3.1.1. Optimisation of initiator concentrations

Gel-MA hydrogels were successfully fabricated using the Ru/SPS photo-initiator system in the 400 - 450nm visible light range. Optimisation of the irradiation conditions required to fabricate Gel-MA hydrogels was investigated by examining a range of initiator concentrations whilst keeping the light intensity constant at 30 mW/cm^2. This was based on previously reported data indicating this light intensity as optimal for protein-protein crosslinking [42,43]. The crosslinking efficiency was measured by the sol fraction (eq 3), which is defined as the weight fraction of polymer chains that are not covalently bound to the hydrogel network after photo-polymerisation [1,44,45]. It was observed that at 0.1/1 Ru/SPS (mM/mM), a minimum of 5 minutes exposure time was required to fabricate stable hydrogels, with resultant sol fraction of approximately 35 - 42% (Figure 2A). Increasing the initiator concentration to 0.2/2 Ru/SPS (mM/mM) significantly increased the polymerisation rate ($p<0.05$), resulting in the fabrication of hydrogels with sol fraction less than 30% within 0.5 min. The sol fraction values decreased as the exposure time increased, and plateaued at

approximately 15%. This minimal sol fraction value achieved was also comparable to gels crosslinked using Vis + 0.05wt% LAP and UV + 0.05wt% I2959 (Fig 2A). Furthermore, increasing the initiator concentration to 0.3/3 Ru/SPS (mM/mM) resulted in identical sol fraction profiles as 0.2/2 Ru/SPS (mM/mM). This result indicates that complete crosslinking of the Gel-MA macromers was achieved using 0.2/2 Ru/SPS (mM/mM). One major observation was that gels crosslinked using UV + 0.05wt% I2959 had a faster polymerisation rate, where the sol fraction value plateaued after 0.5 min of UV exposure.

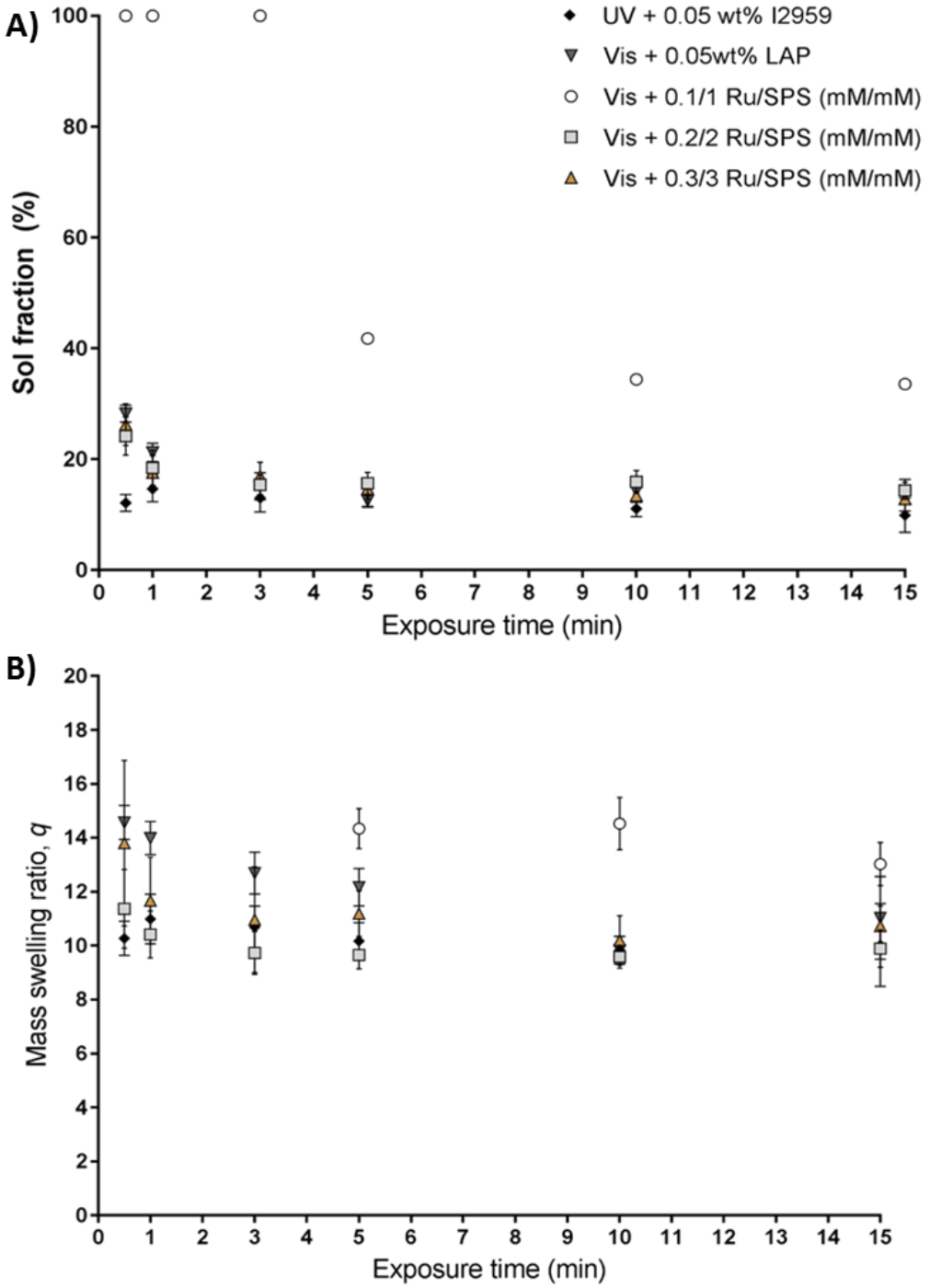

Figure 2: Physico-chemical properties of Gel-MA hydrogels fabricated using different concentrations of Ru/SPS as a function of exposure time: A) Sol fraction; B) Mass swelling ratio, *q*. Gel-MA gels crosslinked using UV + 0.05wt% I2959 and Vis + 0.05wt% LAP were used as controls. Light intensities for both UV and visible (Vis) light were kept constant at 30 mW/cm^2 for 15 minutes. Sol fraction values of 100% indicate no hydrogel formation.

Results obtained for the mass swelling ratio (*q*) complemented the sol-gel analysis, where a decrease in *q* was observed for longer exposure times (Figure 2B). Furthermore, samples with higher sol fraction possessed higher mass swelling ratios. Once again, increasing

the initiator concentration from 0.2/2 Ru/SPS (mM/mM) to 0.3/3 Ru/SPS (mM/mM) did not show any significant differences in the mass swelling ratio (p = 0.9680), demonstrating that 0.2/2 Ru/SPS (mM/mM) was sufficient to completely crosslink the macromers.

3.1.2. Mechanical testing of Gel-MA hydrogels

It was observed that after 15 minutes of exposure at 30 mW/cm^2, Gel-MA hydrogels fabricated using 0.1/1 Ru/SPS (mM/mM) had a compressive modulus of 12.8 ± 1.7 kPa (Figure 3). Increasing the initiator concentration to 0.2/2 Ru/SPS (mM/mM) resulted in hydrogels of significantly greater compressive modulus (31.6 ± 0.8 kPa, p < 0.0001), which were comparable to Gel-MA hydrogels fabricated using the conventional Vis + 0.05wt% LAP (33.5 ± 1.6 kPa, p = 0.5356) and UV + 0.05wt% I2959 (33.6 ± 2.1 kPa, p = 0.4740). However, no significant difference was observed when the initiator concentration was further increased to 0.3/3 Ru/SPS (mM/mM) (29.4 ± 1.9 kPa, p = 0.3626). Again, this result indicated that 0.2/2 Ru/SPS (mM/mM) was sufficient to completely crosslink the Gel-MA macromers, which led to the selection of this concentration for all further studies described herein.

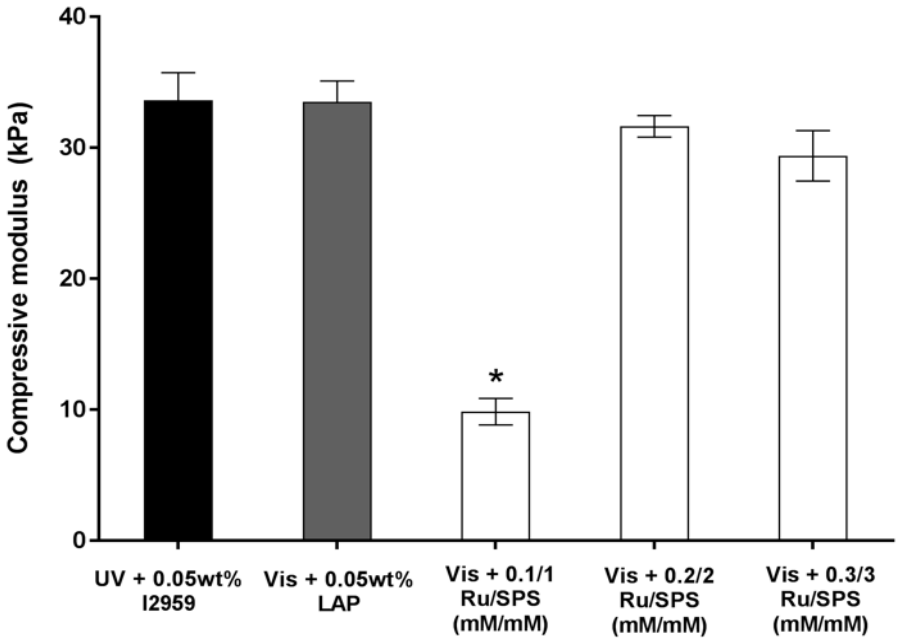

Figure 3: Compressive modulus of Gel-MA hydrogels fabricated using different concentrations of Ru/SPS. Light intensity and irradiation time were kept at 30 mW/cm^2 and 15

minutes, respectively. Gel-MA gels crosslinked using UV + 0.05wt% I2959 and Vis + 0.05wt% LAP were used as controls. *Indicates significant difference to other columns ($p < 0.05$).

3.2. HAC encapsulation in Gel-MA hydrogels

As the overall goal was to investigate the potential for the visible light cross-linking system to be used for 3D cell encapsulation in tissue engineering applications, expanded (passage 2) HACs were encapsulated into the 3D Gel-MA hydrogels. Live-dead fluorescence images following short (1 day) and long-term (35 days) *in vitro* culture showed that the cell-laden gels fabricated using the UV + I2959, Vis + LAP and Vis + Ru/SPS system demonstrated good viability and an abundance of live cells (Figure S1). In a 3D environment, chondrocytes typically exhibit a rounded morphology as an indication of their chondrogenic phenotype [41]. For all time points, it was observed that in all the UV + I2959, Vis + LAP and Vis + Ru/SPS system, the encapsulated cells were not only homogenously distributed, but also remained rounded (Figure S2).

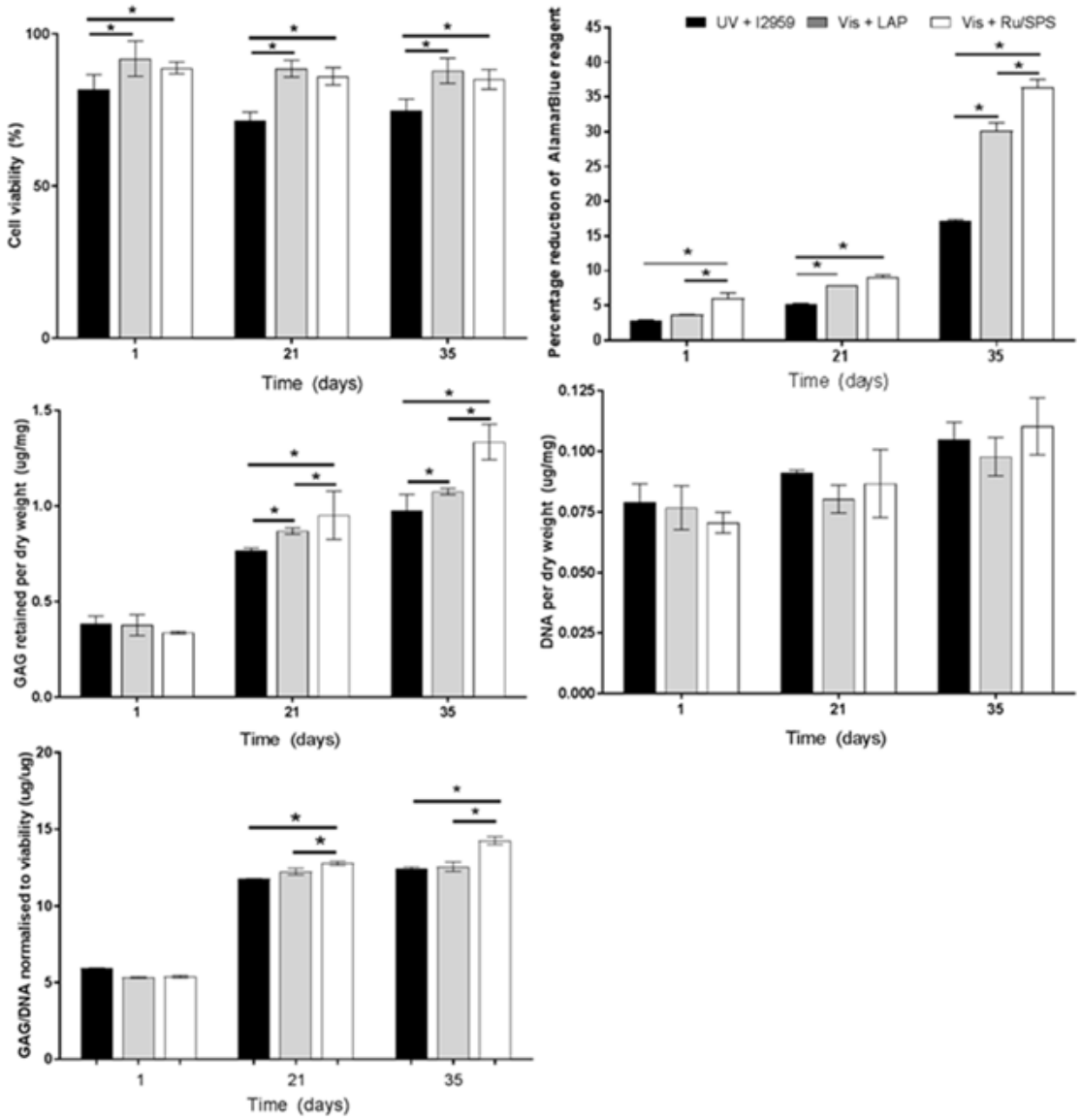

Figure 4: Encapsulation of HACs in Gel-MA hydrogels using UV + I2959, Vis + LAP, and Vis + Ru/SPS, at 1, 21 and 35 days in culture. A) Cell viability (%); B) Metabolic activity reported as percentage reduction of Alamarblue reagent; C) GAG retained per dry weight (µg/mg); D) DNA per dry weight (µg/mg); C) GAG/DNA normalised to cell viability. *Significant differences between columns below each end of lines ($p < 0.05$).

Total live/dead cell counts were used to evaluate viability of the encapsulated HACs. All systems demonstrated good cell viability over the 35-day culture period (>80%). Both the Vis + LAP and Vis + Ru/SPS system showed significantly higher cell viability than the UV + I2959 system for all three examined time points (Figure 4A). We also observed no significant differences between the two systems utilising visible light photo-initiation in terms of cell viability across all time points. After longer-term culture for 35 days, HACs encapsulated using

the UV + I2959 system showed a reduction in viability, whereas cell viability in both the Vis + LAP and Vis + Ru/SPS samples remained greater than 85%. These results suggests that the visible light photo-initiator system presents a more cyto-compatible environment as compared to the UV crosslinking system.

Furthermore, metabolic activity of each of the samples was examined in order to evaluate the biological function of encapsulated cells. It was observed that the Vis + Ru/SPS samples had significantly higher metabolic activity at 1 ($p = 0.0016$), 21 ($p = 0.0001$) and 35 days ($p < 0.0001$) compared to UV + I2959 (Figure 4B). Similarly, the Vis + LAP samples also showed statistically higher metabolic activity compared to gels crosslinked using UV + I2959 at 21 ($p = 0.0146$) and 35 days ($p < 0.0001$). These results indicate that although cells encapsulated in Gel-MA using the conventional UV + I2959 system exhibit favourable cell viability and metabolic activity throughout the culture period, the visible light system showed an improvement on both measures, which was likely due to the lower overall photo-toxicity, radical toxicity and oxidative stress exerted on the cells.

To determine the ability of all UV + I2959, Vis + LAP and Vis + Ru/SPS Gel-MA hydrogels to support biological function and extracellular matrix formation, the chondrogenic differentiation capacity of the HACs post encapsulation was examined *in vitro*. Figure 4D demonstrates that the encapsulated HACs were able to proliferate within the gels, regardless of which photo-initiation system was used, where an increase in DNA content was observed from 1 day to 35 days. However, no significant differences were observed across all three systems at every examined time point. In terms of tissue formation, there was a clear increase in total GAG content from 1 to 35 days in the UV + I2959 ($p < 0.0001$), Vis + LAP ($p < 0.001$) and Vis + Ru/SPS ($p < 0.0001$) constructs (Figure 4C). Both visible light systems resulted in significantly higher GAG content of samples, compared to those crosslinked with the UV + I2959 system at 21 and 35 days. In addition, HACs encapsulated using Vis + Ru/SPS secreted

more GAGs in the hydrogels at 21 (p = 0.0033) and 35 days (p < 0.0001) after encapsulation, compared to the Vis + LAP crosslinked samples.

If we consider the re-differentiation capacity of cell encapsulated Gel-MA constructs, GAG/DNA in the UV + I2959, Vis + LAP and Vis + Ru/SPS samples increased significantly from 1 to 35 days, indicating that these Gel-MA hydrogels are able to support chondrogenic differentiation of HACs (Figure 4E). However, most importantly, we observed that after 35 days in culture, constructs encapsulated using Vis + Ru/SPS had significantly higher GAG/DNA (14.2 ± 0.7 µg/µg) than in the Vis + LAP (12.5 ± 0.9 µg/µg, p < 0.0001) and UV + I2959 system (12.4 ± 0.4 µg/µg, p < 0.0001). Immunofluorescence analysis confirms that the encapsulated HACs secreted collagen type I, collagen type II and aggrecan in the GelMA hydrogels, regardless of the applied photo-encapsulation system. Further quantitative analysis showed that there are no significant differences in terms of collagen type I and collagen type II production within the gels among all three photo-polymerisation systems (Figure 5J and K). However, the total coverage area for aggrecan was significantly higher in the Vis + Ru/SPS as compared to the UV + I2959 and Vis + LAP systems (Figure 5L) where a higher expression of aggrecan was stained in the pericellular regions of the HACs at day 35 in the Vis + Ru/SPS constructs (Figure 5G-I). Chondrogenic gene expressions at early culture time point (day 7) were evaluated to further study the effect of oxidative stress that is exerted on the cells during the photo-encapsulated process. We did observe that the gene expressions for collagen type II and aggrecan are indeed higher in the Vis + Ru/SPS systems (Figure 5M, N & O), further confirming our other observations that this photo-crosslinking system is more cell friendly, and exerts less damage to the cells during the encapsulation process.

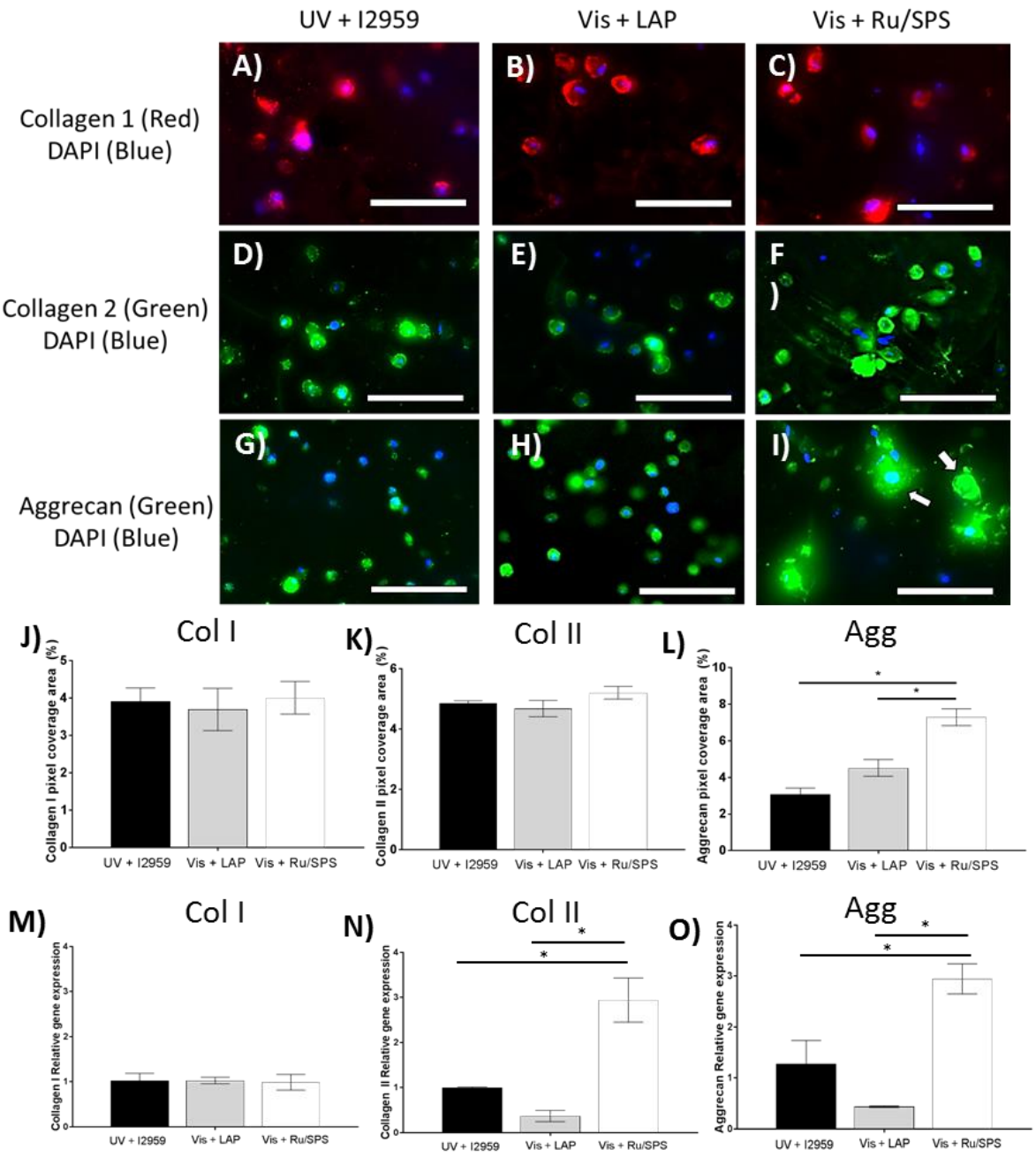

Figure 5: Immunofluorescence staining of HAC encapsulated in Gel-MA hydrogels using UV + I2959, Vis + LAP, or Vis + Ru/SPS after 35 days in culture: collagen type I (A-C); collagen type II (D-F); aggrecan (G-I). Pixel coverage area per panel for collagen I (J), collagen II (K) and aggrecan (L). Early relative gene expression after 7 days in culture: collagen I (M), collagen II (N) and aggrecan (O). Scale bar = 100 µm. *Significant differences between columns below each end of lines ($p < 0.05$).

3.3. Light penetration depth study

As the photo-polymerisation processes can be applied to fabricate *in vivo* injectable hydrogels for tissue engineering applications, we further compared the effectiveness of the photo-polymerisation systems for fabrication of thick hydrogel constructs (10mm). One of the major advantage of using visible light is the better light penetration depth over UV that will be a beneficial for transdermal polymerisation or *in situ* crosslinking. As our cell encapsulation data suggested that the Vis + Ru/SPS is more superior over the Vis + LAP system in terms of HAC metabolic activity and re-differentiation capacity, we chose to only compare the Vis + Ru/SPS to the more conventional UV + I2959 for subsequent experiments. The UV + I2959 system demonstrated a limited penetration depth (6 - 8mm), whereas Vis + Ru/SPS system was able to penetrate through and completely polymerise the entire 10mm thick construct (Figure 6B). This observation was confirmed by mass loss data, where the Vis + Ru/SPS gels of different irradiation depths (i to v) had no significant difference in sol fraction values ($p > 0.98$). In contrast, for the UV + I2959 crosslinked samples, regions of the hydrogel farthest away from the irradiation source exhibited an increased sol fraction, with samples beyond 6mm (regions iv - v) completely dissolving after 1 day (sol fraction = 100%). A similar trend was observed for the mass swelling ratios, where no significant difference was observed for the Vis + Ru/SPS crosslinked samples across all regions (i to v). However, gels crosslinked using the UV + I2959 had distinctly different swelling ratios at different depths from the irradiation source (Figure 6D). These results further indicated that UV light has limited penetration depth as well as being attenuated through the z-axis during photo-crosslinking, resulting in varying crosslinking density with depth within the hydrogel.

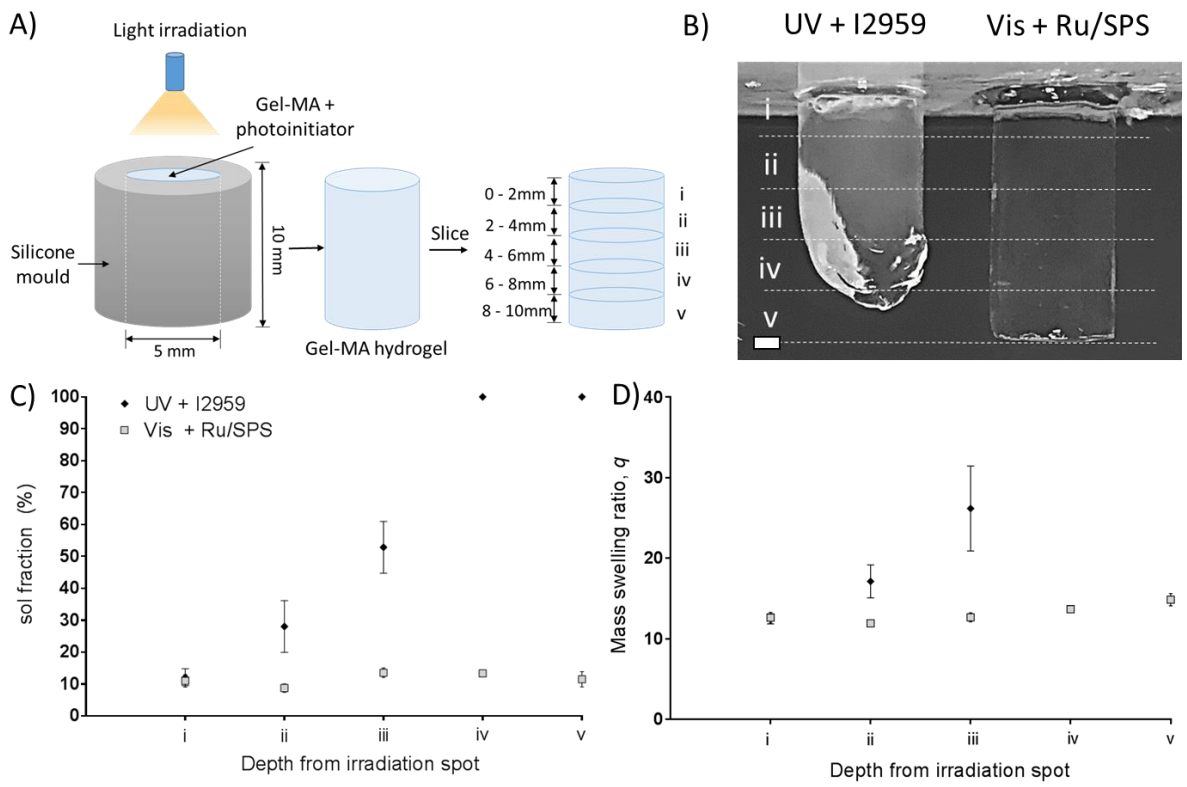

Figure 6: Fabrication of thick hydrogel constructs using both UV + I2959 and Vis + Ru/SPS systems: A) Schematic of light penetration depth setup; B) Macroscopic images of Gel-MA constructs post photo-polymerisation, scale bar = 1 mm; C) Sol fraction values; and D) Mass swelling ratios of samples as per depth from irradiation spot.

We further extended our studies to evaluate cell viability within the samples at different depths from the irradiation source (Figure 7). Interestingly, we observed an increase in cell viability at increasing depths for the UV crosslinked samples, where cells in the middle regions (iii, 4 – 6 mm from the irradiation source) had significantly higher viability ($p < 0.0001$) than those cells closer to the light source (i, < 2 mm from irradiation source). This data concurs with our previous mass loss results (Figure 6C), where UV light was likely being attenuated through the z-axis, with cells at different irradiation depths being subjected to different UV light intensity. In contrast, no significant differences in cell viability were observed for the Vis + Ru/SPS samples throughout the full 10mm depth of the construct (regions i-v)

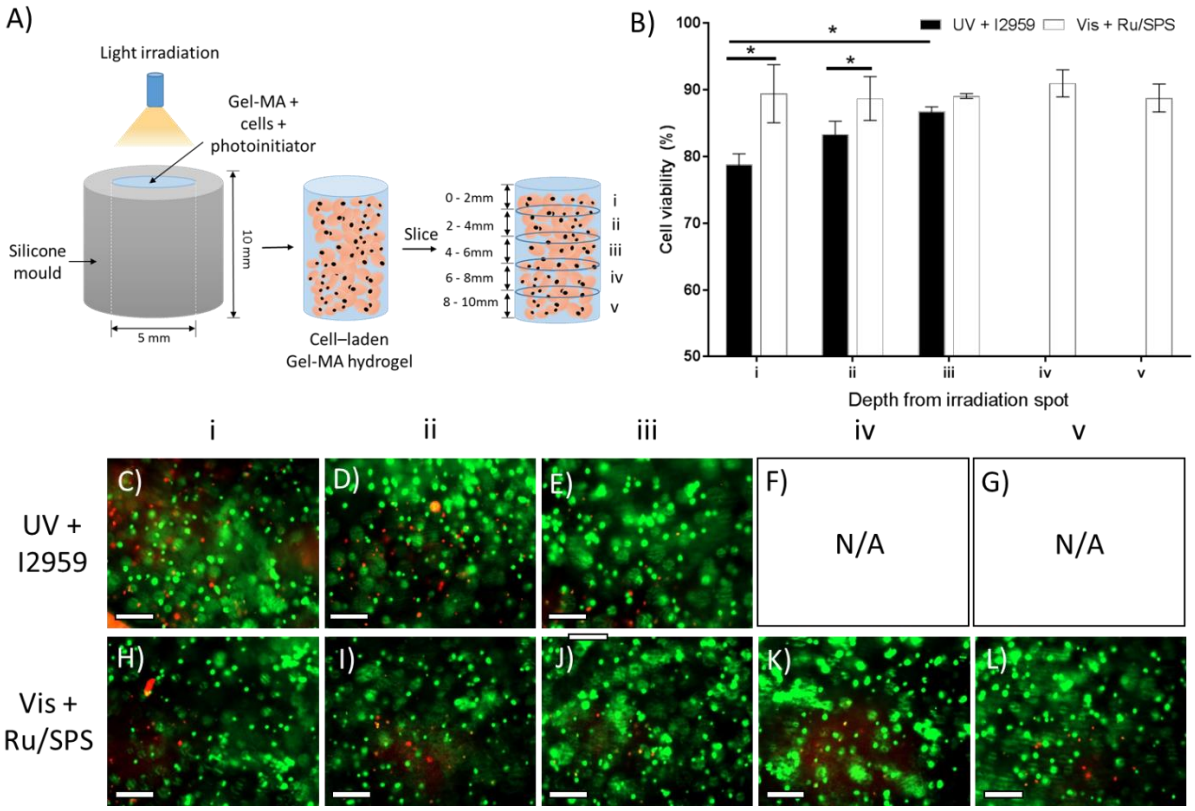

Figure 7: Fabrication of thick cell-laden constructs using both UV + I2959 and Vis + Ru/SPS systems: A) Schematic of light penetration depth setup; B) Cell viability at different depths from the light irradiation spot. Live dead images of UV + I2959 crosslinked samples (C - G) for different irradiation depths i, ii, iii, iv and v respectively, scale bar = 100 µm. Images F and G were not available due to the gels completely dissolved after 1 day in culture. Live dead images of Vis + Ru/SPS crosslinked samples (H - L) for different irradiation depths i, ii, iii, iv and v respectively, scale bar = 100 µm.

3.4. Transdermal polymerisation study and *in vivo* subcutaneous implantation

One of the major advantages of having a greater light penetration depth is the potential use of this visible light photo-crosslinking system for transdermal polymerisation. We evaluated the possibility to fabricate hydrogels transdermally using murine skin (0.5 mm) as a model (Figure 8A), and observed that UV light had limited transmission through skin resulting in the formation of a weak gel that was completely dissolved after 1day (100% sol fraction, Figure 8B). In contrast, hydrogels were successfully crosslinked using visible light transmitted through the murine skin, with no statistically difference in sol fraction and swelling ratio to the control (Figure 8B). *In vivo* studies showed that after 14 days of subcutaneous implantation,

there was limited cell infiltration into the hydrogels fabricated using both the UV + I2959 and Vis + Ru/SPS system. No significant differences were observed in terms of the host response to the gels fabricated using both these systems, again suggesting that there were no distinct differences in physico-chemical and mechanical properties of hydrogels crosslinked using either UV + I2959 or Vis + Ru/SPS, and is in agreement with our *in vitro* data.

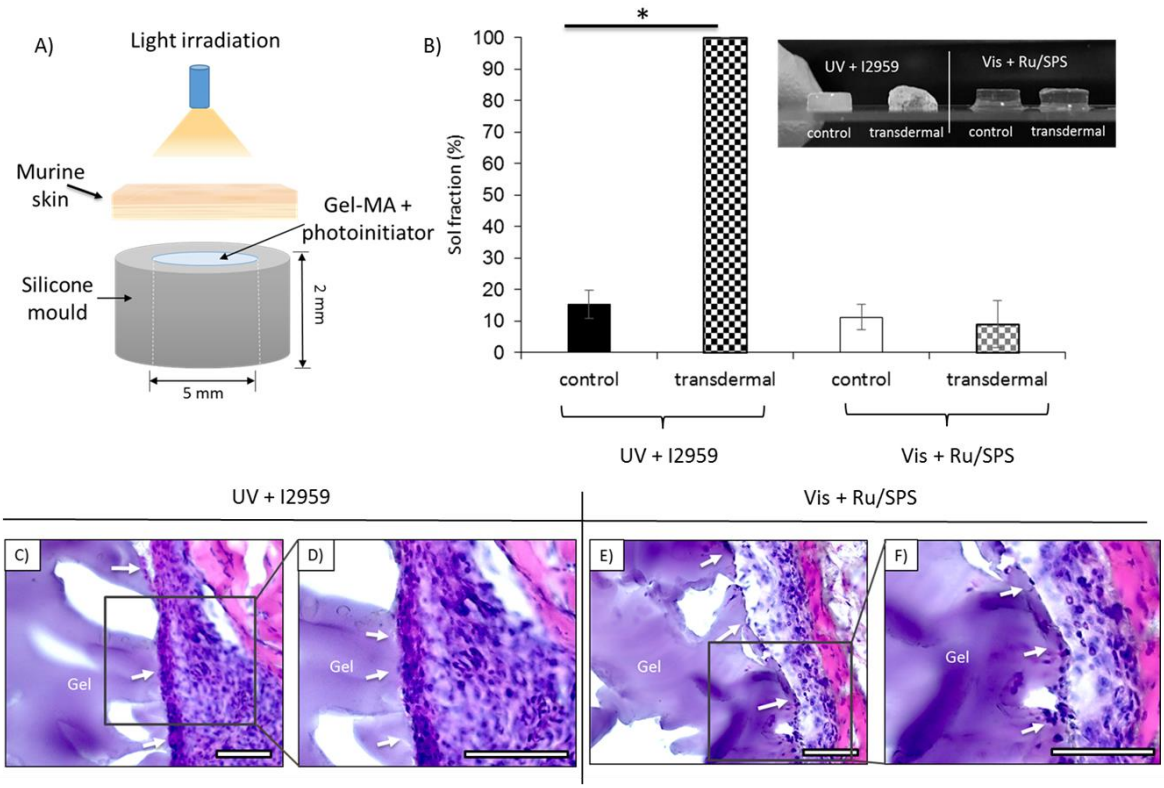

Figure 8: Transdermal polymerisation of Gel-MA constructs using both UV + I2959 and Vis + Ru/SPS systems: Schematic (A) and sol fraction (B) of Gel-MA hydrogels photo-crosslinked using light transmitted through murine skin; Immunohistochemical staining (H&E) of Gel-MA hydrogels fabricated using UV + I2959 (C & D) and Vis + Ru/SPS (E & F) post 14 days implanted subcutaneously. White arrows pointing to hydrogel and tissue interface. Scale bar = 100 µm.

4. Discussion

In this study, we demonstrated that the optimal irradiation conditions to fabricate Gel-MA hydrogels consisted of a visible light intensity of 30 mW/cm^2, photo-initiator concentration of 0.2/2 Ru/SPS (mM) and at least 3 minutes of exposure time. However more importantly, it should be recognised that the Ru/SPS concentration required to fully photo-crosslink Gel-MA

hydrogels in this study was 10 times lower than the initiator concentrations reported to date in the literature to crosslink other polymers via their phenol moieties [4,46,47]. This difference in initiator concentrations between Gel-MA and the other phenolated polymers such as gelatin, fibrinogen, resilin and tyraminated PVA, may likely be due to the reactivity of different functional groups, as well as different initiator components that are responsible for crosslinking. During the photo-polymerisation process, Ru^{2+} is photo-excited to Ru^{3+} by donating electrons to SPS [35,48]. For other phenolated polymeric systems, Ru^{3+} is responsible for the crosslink formation. However in our case, the sulphate radicals which are products from the dissociation of SPS are responsible for reacting with methacryloyl groups on Gel-MA to form covalent crosslinks. As the reaction between the sulphate radicals and the methacryloyl groups is more effective than the reaction between the Ru^{3+} and phenol groups, less Ru/SPS is therefore required to crosslink the Gel-MA hydrogels. On the other hand, however, the Ru^{3+} component may contribute to crosslinking the phenol groups present in the gelatin backbone concurrently.

The sol fraction (10 – 15%), mass swelling ratio q (9 – 10) and compressive moduli (~20 kPa) obtained for Vis + 0.2/2 Ru/SPS (mM/mM) Gel-MA hydrogels in this study are comparable to properties obtained for Gel-MA gels fabricated using the UV + I2959 and Vis + LAP systems [49,50]. This result indicates that the visible light system is capable of fabricating Gel-MA hydrogels of equivalent physico-mechanical properties to the other more conventional and widely adopted photo-initiated polymerisation system. Although we did observe that the UV + I2959 system had a faster crosslinking rate compared to both the Vis + LAP and Vis + Ru/SPS systems, the mass loss and swelling studies were conducted in an ideal environment without taking oxygen inhibition and light penetration depth into account, where the macromer was irradiated while sandwiched between a glass slide and cover slip, and is not an accurate representation of the downstream application. Moreover, in addition to Gel-MA

hydrogels alone, we have successfully employed this visible light system to other polymers including heparin, hyaluronic acid, poly(vinyl alcohol) and gellan gum, all of which were functionalised with unsaturated vinyl moieties, such as methacryloyl or allyl groups [36,38,51]. Taking these factors into account, our work suggests that both synthetic and biological polymers modified with functional vinyl moieties can be crosslinked through different chemistries such as chain-growth methacryloyl or step-growth thiol-ene photo-click polymerisation, using Vis + Ru/SPS.

As expected, encapsulated cells had high cell viability (>80%) after 1 day for both photoinitiator systems. This result is comparable to a previous study reported by Schuurman *et al.* where after 1 day, the viability of equine articular chondrocytes encapsulated in 10wt% Gel-MA gels crosslinked using UV + I2959 was approximately 83% [52]. Nichol *et al.* also showed that fibroblasts encapsulated in 10wt% Gel-MA gels had viability of 82% after UV polymerisation [49]. In this study, applying either the Vis + LAP or Vis + Ru/SPS system resulted in cell-laden hydrogel constructs with an improved cell viability and significantly higher metabolic activity than UV gels. We believe that this result might be due to the negative effect of UV irradiation to the cells, which has been shown to cause genomic instability of cells [38,53,54]. Previous work from Greene *et al.* describes that hepatocytes photo-encapsulated in gelatin-norbornene gels using visible light + eosin-Y had significantly higher metabolic activity compared to their UV counterparts [14]. Caliari *et al.* also showed that UV irradiation significantly reduced the cell viability of hepatic stellate cells when compared to visible light for encapsulation in methacrylated hyaluronic acid hydrogels [55]. Furthermore, UV is known to react with oxygen in the environment, forming reactive oxygen species (ROS) such as superoxide radical ($O_2^{\cdot -}$), hydroxyl radical ($OH^{\cdot}$), singlet oxygen ($^1O_2$) and ozone (O_3), which can oxidise the lipid bilayer of cells [54,56,57]. This lipid peroxidation may disrupt the cell membrane integrity and permeability, which can lead to upregulation of tissue degrading

enzymes, and generation of toxic products [54,57]. The chondrogenic differentiation study showed that GAG content and re-differentiation capacity (GAG/DNA) of HACs were significantly higher in the Vis + Ru/SPS samples than their Vis + LAP and UV + I2959 counterparts after long-term 35 day culture. As both LAP and Ru/SPS require visible light for photo-initiation, the difference observed in cell viability, metabolic activity and re-differentiation capacity, might be due to the diverse radical generation mechanism. We hypothesise that the Ru + SPS system has a slower but more sustained radical generation rate being a non-cleavage type 2 photoinitiator that undergoes a self-recycling mechanism (Figure 1) [35,39,48,58]. It has been previously reported that this ability to re-initiate polymerisation allows type 2 photoinitiators to be less affected by oxygen inhibition [58]. Further covalent incorporation of chondrogenic factors or growth factor-binding peptides within Vis + Ru/SPS Gel-MA hydrogels (such as TGF-ß1, hyaluronic acid, heparin) would likely further enhance this chondrogenic niche [12,59].

The clinical relevance of these visible light initiating systems are particularly appealing for cell delivery or as space-fillers post augmentation, where *in situ* photo-curing typically requires high light intensity to minimise both oxygen inhibition and light attenuation. We demonstrated that the UV + I2959 system has a limited light penetration depth and can be attenuated during photo-crosslinking of constructs greater than 2 mm in thickness. Although a maximum penetration depth of 6 mm could be achieved with UV, variations in physical properties (sol fraction and mass swelling ratio) and cell viability were detected, indicating an inhomogeneous and sub-optimal crosslinking density throughout the construct. Our findings correlate to previous studies which also highlighted the limited penetration depth of UV light in either photo-curing of dental resin [60], photo-responsive polymers [61,62] or transdermal photo-polymerisation [23]. The Vis + Ru/SPS system showed an added advantage in having enhanced penetration depth with homogenous crosslinking density and cell viability

throughout a 10 mm thick construct. Furthermore, we have also reported that the Vis + Ru/SPS system is less susceptible to oxygen inhibition compared to the UV + I2959 system, allowing fabrication of large 3D bioprinted constructs with good shape fidelity [39]. In a transdermal polymerisation setup, we observed that a visible light intensity of 30 mW/cm^2 was enough to transmit through the murine skin and enable photo-crosslinking of the Gel-MA + 0.2/2 (mM/mM) Ru/SPS macromer. In contrast, using the same UV intensity and 0.05wt% I2959 did not result in successful hydrogel fabrication, highlighting the limited skin penetration and transmittance of light in the UV range. Lin *et al.* previously showed that a combination of higher UV intensity (40 mW/cm^2) and I2959 concentration (0.5wt%) was indeed able to facilitate transdermal polymerisation of Gel-MA hydrogels [63]. However, we showed that the Vis + Ru/SPS system is significantly more efficient where lower visible light intensity and Ru/SPS concentrations were sufficient to transdermally fabricate hydrogels of similar quality to the controls. Although the murine skin model (0.5 mm) used in this study is thinner, it does consist of three distinctive layers (epidermis, dermis and hypodermis) similarly to human skin (1 – 2 mm). The cytotoxicity of the transition metal Ru might raise some concerns for use in clinical applications. Therefore, we conducted a cell growth inhibition assay to assess the toxicity of Ru in accordance to the ISO10993 standard. We observed that the concentration of Ru (0.2 mM) used in this study is below the accepted cytotoxicity threshold (<30%, Fig S1). This result is in agreement with a previous study conducted by Elvin *et al.*, where even a concentration as high as 1 mM of Ru was not cytotoxic [10]. In the same study, Elvin *et al.* also showed that gelatin-tyramines were fabricated into tissue sealants using 1/20 Ru/SPS (mM/mM) and showed minimal inflammatory response and no adverse cytotoxic reactions based on histological analysis [10]. Similarly, our *in vivo* subcutaneous study also displayed that the Gel-MA hydrogels fabricated using Vis + Ru/SPS showed no significant difference in host tissue reaction in comparison to the UV + I2959 counterparts (Figure 8C-F).

We believe that adopting the Vis + Ru/SPS system offers advantages over the UV irradiation system with respect to not only promoting cell viability and function within *in situ* photo-cured hydrogels or 3D constructs, but importantly to host cells in surrounding healthy issue that would also be exposed to high light intensity, particularly during the photo-polymerisation of thick or large constructs. Furthermore, we purport that the applicability of the Vis + Ru/SPS system may be of particular benefit over Vis + LAP and UV + I2959 systems in the field of biofabrication or 3D bioprinting of thick, cell-laden constructs, where again, high light intensity or high photo-initiator concentration are generally necessary to maintain shape fidelity of biofabricated constructs as well as obtain maximum cell survival [39].

5. Conclusions

We have demonstrated and optimised the use of the visible light photo-initiators (Ru/SPS) to fabricate Gel-MA hydrogels. The fabricated gels offered similar physico-chemical and mechanical properties compared to those crosslinked using conventionally adopted UV + I2959 photo-initiator system. HACs encapsulated in visible light polymerised gels demonstrated superior cell viability and metabolic activity, as well as greater GAG content and re-differentiation capacity (GAG/DNA) as compared to UV crosslinked Gel-MA hydrogels. Furthermore, the enhanced penetration depth observed for the visible light system offers added benefits for *in situ* photo-curing applications and fabrication of thick hydrogel constructs. This study highlights the potential of this Vis + Ru/SPS system for fabrication of Gel-MA gels for not only cartilage engineering, but also other tissue engineering applications including cell delivery and *in-situ* photo-curing.

Acknowledgements

The authors wish to acknowledge Dr Ben Schon for his scientific input and his involvement in the subcutaneous implantation study. The authors also wish to acknowledge

funding support from the Royal Society of New Zealand Rutherford Discovery Fellowship (RDF-UOO1204; TW), Health Research Council of New Zealand Emerging Researcher First Grant and Sir Charles Hercus Fellow (HRC 15/483 & 19/135; KL), the EU/FP7 'skelGEN' consortium under grant agreement n° [318553], the Dutch Arthritis Foundation (LLP-12; JM) and the European Research Council under grant agreement 647426 (3D-JOINT; JM).

References

[1] Lim K S, Roberts J J, Alves M-H, Poole-Warren L A and Martens P J 2015 Understanding and tailoring the degradation of PVA-tyramine hydrogels *J. Appl. Polym. Sci.* **132** 42142

[2] Nafea E H, Poole-Warren L A and Martens P J 2014 Structural and permeability characterization of biosynthetic PVA hydrogels designed for cell-based therapy *J. Biomater. Sci. Polym. Ed.* **25** 1771–90

[3] Schon B S, Hooper G J and Woodfield T B F 2016 Modular Tissue Assembly Strategies for Biofabrication of Engineered Cartilage *Ann. Biomed. Eng.* **45** 100–14

[4] Lim K S, Alves M H, Poole-Warren L A and Martens P J 2013 Covalent incorporation of non-chemically modified gelatin into degradable PVA-tyramine hydrogels *Biomaterials* **34** 7907–105

[5] Bryant S, Nicodemus G and Villanueva I 2008 Designing 3D Photopolymer Hydrogels to Regulate Biomechanical Cues and Tissue Growth for Cartilage Tissue Engineering *Pharm. Res.* **25** 2379–86

[6] Van Den Bulcke A I, Bogdanov B, De Rooze N, Schacht E H, Cornelissen M and Berghmans H 2000 Structural and Rheological Properties of Methacrylamide Modified Gelatin Hydrogels *Biomacromolecules* **1** 31–8

[7] Manabe T, Okino H, Tanaka M and Matsuda T 2004 In situ-formed, tissue-adhesive co-gel composed of styrenated gelatin and styrenated antibody: potential use for local anti-cytokine antibody therapy on surgically resected tissues *Biomaterials* **25** 5867–73

[8] Vuocolo T, Haddad R, Edwards G A, Lyons R E, Liyou N E, Werkmeister J A, Ramshaw J A M and Elvin C M 2012 A Highly Elastic and Adhesive Gelatin Tissue Sealant for Gastrointestinal Surgery and Colon Anastomosis *J. Gastrointest. Surg.* **16** 744–52

[9] Hoshikawa A, Nakayama Y, Matsuda T, Oda H, Nakamura K and Mabuchi K 2006 Encapsulation of chondrocytes in photopolymerizable styrenated gelatin for cartilage tissue engineering *Tissue Eng.* **12** 2333–41

[10] Elvin C M, Vuocolo T, Brownlee A G, Sando L, Huson M G, Liyou N E, Stockwell P R, Lyons R E, Kim M, Edwards G A, Johnson G, McFarland G A, Ramshaw J A M and Werkmeister J A 2010 A highly elastic tissue sealant based on photopolymerised gelatin *Biomaterials* **31** 8323–31

[11] Melchels F P W, Dhert W J A, Hutmacher D W and Malda J 2014 Development and characterisation of a new bioink for additive tissue manufacturing *J. Mater. Chem. B* **2** 2282–9

[12] Brown G C J, Lim K S, Farrugia B L, Hooper G J and Woodfield T B F 2017 Covalent Incorporation of Heparin Improves Chondrogenesis in Photocurable Gelatin-Methacryloyl Hydrogels *Macromol. Biosci.* **17** 1700158

[13] Klotz B J, Gawlitta D, Rosenberg A J W P, Malda J and Melchels F P W 2016 Gelatin-Methacryloyl Hydrogels: Towards Biofabrication-Based Tissue Repair *Trends Biotechnol.* **34** 394–407

[14] Greene T, Lin T, Ourania M A and Lin C 2016 Comparative study of visible light polymerized gelatin hydrogels for 3D culture of hepatic progenitor cells *J. Appl. Polym. Sci.* **134** 44585

[15] Bryant S J, Nuttelman C R and Anseth K S 2000 Cytocompatibility of UV and visible light photoinitiating systems on cultured NIH/3T3 fibroblasts in vitro *J. Biomater. Sci. Polym. Ed.* **11** 439–57

[16] de Gruijl F R, van Kranen H J and Mullenders L H F 2001 UV-induced DNA damage, repair, mutations and oncogenic pathways in skin cancer *J. Photochem. Photobiol. B Biol.* **63** 19–27

[17] Dahle J and Kvam E 2003 Induction of Delayed Mutations and Chromosomal Instability in Fibroblasts after UVA-, UVB-, and X-Radiation *Cancer Res.* **63** 1464–9

[18] Dahle J, Kvam E and Stokke T 2005 Bystander effects in UV-induced genomic instability: antioxidants inhibit delayed mutagenesis induced by ultraviolet A and B radiation *J. Carcinog.* **4** 11

[19] Lavker R and Kaidbey K 1997 The Spectral Dependence for UVA-Induced Cumulative Damage in Human Skin *J. Invest. Dermatol.* **108** 17–21

[20] Urushibara A, Kodama S and Yokoya A 2014 Induction of genetic instability by transfer of a UV-A-irradiated chromosome *Mutat. Res. Toxicol. Environ. Mutagen.* **766** 29–34

[21] Peak J G and Peak M J 1991 Comparison of initial yields of DNA-to-protein crosslinks and single-strand breaks induced in cultured human cells by far- and near-ultraviolet light, blue light and X-rays *Mutat. Res. Mol. Mech. Mutagen.* **246** 187–91

[22] Cooke M S, Evans M D, Dizdaroglu M and Lunec J 2003 Oxidative DNA damage: mechanisms, mutation, and disease *FASEB J.* **17** 1195–214

[23] Elisseeff J, Anseth K, Sims D, McIntosh W, Randolph M and Langer R 1999 Transdermal photopolymerization for minimally invasive implantation *Proc. Natl. Acad. Sci. U. S. A.* **96** 3104–7

[24] Hu J, Hou Y, Park H, Choi B, Hou S, Chung A and Lee M 2012 Visible light crosslinkable chitosan hydrogels for tissue engineering *Acta Biomater.* **8** 1730–8

[25] Jakubiak J, Allonas X, Fouassier J P, Sionkowska A, Andrzejewska E, Linden L Å and Rabek J F 2003 Camphorquinone–amines photoinitating systems for the initiation

of free radical polymerization *Polymer (Guildf).* **44** 5219–26

[26] Mazaki T, Shiozaki Y, Yamane K, Yoshida A, Nakamura M, Yoshida Y, Zhou D, Kitajima T, Tanaka M and Ito Y 2014 A novel, visible light-induced, rapidly cross-linkable gelatin scaffold for osteochondral tissue engineering *Sci. Rep.* **4** 4457

[27] Fairbanks B D, Schwartz M P, Bowman C N and Anseth K S 2009 Photoinitiated polymerization of PEG-diacrylate with lithium phenyl-2,4,6-trimethylbenzoylphosphinate: polymerization rate and cytocompatibility *Biomaterials* **30** 6702–7

[28] Lin H, Zhang D, Alexander P G, Yang G, Tan J, Cheng A W-M and Tuan R S 2013 Application of Visible Light-based Projection Stereolithography for Live Cell-Scaffold Fabrication with Designed Architecture *Biomaterials* **34** 331–9

[29] Shih H and Lin C C 2013 Visible-light-mediated thiol-ene hydrogelation using eosin-Y as the only photoinitiator *Macromol Rapid Commun* **34** 269–73

[30] Bahney C S, Lujan T J, Hsu C W, Bottlang M, West J L and Johnstone B 2011 Visible Light Photoinitiation of Mesenchymal Stem Cell-laden Biorepsonsive Hydrogels *Eur. Cells Mater.* **22** 43–55

[31] Pelin E, Fidan S, Tugba B and Seda K 2018 Gelatin Methacryloyl Hydrogels in the Absence of a Crosslinker as 3D Glioblastoma Multiforme (GBM)- Mimetic Microenvironment *Macromol. Biosci.* **18** 1700369

[32] Noshadi I, Walker B W, Portillo-Lara R, Shirzaei Sani E, Gomes N, Aziziyan M R and Annabi N 2017 Engineering Biodegradable and Biocompatible Bio-ionic Liquid Conjugated Hydrogels with Tunable Conductivity and Mechanical Properties *Sci. Rep.* **7** 4345

[33] Annabi N, Rana D, Shirzaei Sani E, Portillo-Lara R, Gifford J L, Fares M M, Mithieux S M and Weiss A S 2017 Engineering a sprayable and elastic hydrogel adhesive with antimicrobial properties for wound healing *Biomaterials* **139** 229–43

[34] Lim K S, Ramaswamy Y, Roberts J J, Alves M-H, Poole-Warren L A and Martens P J 2015 Promoting Cell Survival and Proliferation in Degradable Poly(vinyl alcohol)-Tyramine Hydrogels *Macromol. Biosci.* **15** 1423–32

[35] Fancy D A, Denison C, Kim K, Xie Y, Holdeman T, Amini F and Kodadek T 2000 Scope, limitations and mechanistic aspects of the photo-induced cross-linking of proteins by water-soluble metal complexes *Chem. Biol.* **7** 697–708

[36] Lim K S, Levato R, Costa P F, Castilho M D, Alcala-Orozco C R, Dorenmalen K M A van, Melchels F P W, Gawlitta D, Hooper G J, Malda J and Woodfield T B F 2018 Bio-resin for high resolution lithography-based biofabrication of complex cell-laden constructs *Biofabrication* **10** 34101

[37] Muller P and Brettel K 2012 [Ru(bpy)3]2+ as a reference in transient absorption spectroscopy: differential absorption coefficients for formation of the long-lived 3MLCT excited state *Photochem. Photobiol. Sci.* **11** 632–6

[38] Bertlein S, Brown G C J, Lim K S, Jungst T, Boeck T, Blunk T, Tessmar J, Hooper G J, Woodfield T B F and Groll J 2017 Thiol–Ene Clickable Gelatin: A Platform Bioink

for Multiple 3D Biofabrication Technologies *Adv. Mater.* **29** 1703404

[39] Lim K S, Schon B S, Mekhileri N V, Brown G C J, Chia C M, Prabakar S, Hooper G J and Woodfield T B F 2016 New Visible-Light Photoinitiating System for Improved Print Fidelity in Gelatin-Based Bioinks *ACS Biomater. Sci. Eng.* **2** 1752–62

[40] Woodfield T B F, Van Blitterswijk C A, De Wijn J, Sims T J, Hollander A P and Riesle J 2005 Polymer scaffolds fabricated with pore-size gradients as a model for studying the zonal organization within tissue-engineered cartilage constructs *Tissue Eng.* **11** 1297–311

[41] Schrobback K, Klein T J and Woodfield T B 2015 The importance of connexin hemichannels during chondroprogenitor cell differentiation in hydrogel versus microtissue culture models *Tissue Eng Part A* **21** 1785–94

[42] Elvin C M, Brownlee A G, Huson M G, Tebb T A, Kim M, Lyons R E, Vuocolo T, Liyou N E, Hughes T C, Ramshaw J A M and Werkmeister J A 2009 The development of photochemically crosslinked native fibrinogen as a rapidly formed and mechanically strong surgical tissue sealant *Biomaterials* **30** 2059–65

[43] Elvin C M, Carr A G, Huson M G, Maxwell J M, Pearson R D, Vuocolo T, Liyou N E, Wong D C C, Merritt D J and Dixon N E 2005 Synthesis and properties of crosslinked recombinant pro-resilin *Nature* **437** 999–1002

[44] Martens P and Anseth K S 2000 Characterization of hydrogels formed from acrylate modified poly(vinyl alcohol) macromers *Polymer (Guildf).* **41** 7715–22

[45] Roberts J J, Naudiyal P, Lim K S, Poole-Warren L A and Martens P J 2016 A comparative study of enzyme initiators for crosslinking phenol-functionalized hydrogels for cell encapsulation *Biomater. Res.* **20**

[46] Sando L, Danon S, Brownlee A G, McCulloch R J, Ramshaw J A M, Elvin C M and Werkmeister J A 2011 Photochemically crosslinked matrices of gelatin and fibrinogen promote rapid cell proliferation *J. Tissue Eng. Regen. Med.* **5** 337–46

[47] Sando L, Kim M, Colgrave M L, Ramshaw J A M, Werkmeister J A and Elvin C M 2010 Photochemical crosslinking of soluble wool keratins produces a mechanically stable biomaterial that supports cell adhesion and proliferation *J. Biomed. Mater. Res. - Part A* **95** 901–11

[48] Fancy D A and Kodadek T 1999 Chemistry for the analysis of protein–protein interactions: rapid and efficient cross-linking triggered by long wavelength light *Proc Natl Acad Sci U S A* **96** 6020–4

[49] Nichol J W, Koshy S T, Bae H, Hwang C M, Yamanlar S and Khademhosseini A 2010 Cell-laden microengineered gelatin methacrylate hydrogels *Biomaterials* **31** 5536–44

[50] Schuurman W, Khristov V, Pot M W, van Weeren P R, Dhert W J and Malda J 2011 Bioprinting of hybrid tissue constructs with tailorable mechanical properties *Biofabrication* **3** 21001

[51] Parrish J, Lim K S, Baer K, Hooper G J and Woodfield T 2018 A 96-Well Microplate Bioreactor Platform Supporting Individual Dual Perfusion and High-Throughput

Assessment of Simple or Biofabricated 3D Tissue Models *Lab Chip* **18** 2757–75

[52] Schuurman W, Levett P A, Pot M W, van Weeren P R, Dhert W J A, Hutmacher D W, Melchels F P W, Klein T J and Malda J 2013 Gelatin-Methacrylamide Hydrogels as Potential Biomaterials for Fabrication of Tissue-Engineered Cartilage Constructs *Macromol. Biosci.* **13** 551–61

[53] Clydesdale G J, Dandie G W and Muller H K 2001 Ultraviolet light induced injury: Immunological and inflammatory effects *Immunol Cell Biol* **79** 547–68

[54] Halliwell B and Chirico S 1993 Lipid peroxidation: its mechanism, measurement, and significance *Am. J. Clin. Nutr.* **57** 715S–724S

[55] Caliari S R, Perepelyuk M, Cosgrove B D, Tsai S J, Lee G Y, Mauck R L, Wells R G and Burdick J A 2016 Stiffening hydrogels for investigating the dynamics of hepatic stellate cell mechanotransduction during myofibroblast activation *Sci. Rep.* **6** 21387

[56] El-Beltagi H S and Mohamed H I 2013 Reactive Oxygen Species, Lipid Peroxidation and Antioxidative Defense Mechanism *Not Bot Horti Agrobo* **41** 44–57

[57] Greenberg M E, Li X-M, Gugiu B G, Gu X, Qin J, Salomon R G and Hazen S L 2008 The Lipid Whisker Model of the Structure of Oxidized Cell Membranes *J. Biol. Chem.* **283** 2385–96

[58] Kaastrup K and Sikes H D 2016 Using photo-initiated polymerization reactions to detect molecular recognition *Chem. Soc. Rev.* **45** 532–45

[59] Levett P A, Melchels F P W, Schrobback K, Hutmacher D W, Malda J and Klein T J 2014 A biomimetic extracellular matrix for cartilage tissue engineering centered on photocurable gelatin, hyaluronic acid and chondroitin sulfate *Acta Biomater.* **10** 214–23

[60] Santini A, Gallegos I T and Felix C M 2013 Photoinitiators in Dentistry: A Review *Prim. Dent. J.* **2** 30–3

[61] Kloxin A M, Tibbitt M W, Kasko A M, Fairbairn J A and Anseth K S 2010 Tunable Hydrogels for External Manipulation of Cellular Microenvironments through Controlled Photodegradation *Adv. Mater.* **22** 61–6

[62] Wang D, Wagner M, Butt H-J and Wu S 2015 Supramolecular hydrogels constructed by red-light-responsive host-guest interactions for photo-controlled protein release in deep tissue *Soft Matter* **11** 7656–62

[63] Lin R-Z, Chen Y-C, Moreno-Luna R, Khademhosseini A and Melero-Martin J M 2013 Transdermal regulation of vascular network bioengineering using a photopolymerizable methacrylated gelatin hydrogel *Biomaterials* **34** 6785–96